(4-Nitrophenyl)methyl 2,3-dihydro-1*H*-pyrrole-1-carboxylate: crystal structure and Hirshfeld analysis

Julio Zukerman-Schpector, Monica Soto-Monsalve, Regina H. De Almeida Santos, Ariel L. L. Garcia, Carlos Roque D. Correia, Mukesh M. Jotani and Edward R. T. Tiekink

(4-Nitrophenyl)methyl 2,3-dihydro-1H-pyrrole-1-carboxylate: crystal structure and Hirshfeld analysis

Julio Zukerman-Schpector,[a]* Monica Soto-Monsalve,[b] Regina H. De Almeida Santos,[b] Ariel L. L. Garcia,[c] Carlos Roque D. Correia,[c] Mukesh M. Jotani[d] and Edward R. T. Tiekink[e]‡

[a]Laboratório de Cristalografia, Esterodinâmica e Modelagem Molecular, Departamento de Química, Universidade Federal de São Carlos, 13565-905 São Carlos, SP, Brazil, [b]Instituto de Química de São Carlos, Universidade de São Paulo, São Carlos, SP, Brazil, [c]Instituto de Química, Universidade Estadual de Campinas, UNICAMP, CP 6154, CEP. 13084-971, Campinas, São Paulo, Brazil, [d]Department of Physics, Bhavan's Sheth R. A. College of Science, Ahmedabad, Gujarat 380 001, India, and [e]Centre for Crystalline Materials, School of Science and Technology, Sunway University, 47500 Bandar Sunway, Selangor Darul Ehsan, Malaysia. *Correspondence e-mail: julio@power.ufscar.br

In the title compound, $C_{12}H_{12}N_2O_4$, the dihydropyrrole ring is almost planar (r.m.s. deviation = 0.0049 Å) and is nearly coplanar with the adjacent C_2O_2 residue [dihedral angle = 4.56 (9)°], which links to the 4-nitrobenzene substituent [dihedral angle = 4.58 (8)°]. The molecule is concave, with the outer rings lying to the same side of the central C_2O_2 residue and being inclined to each other [dihedral angle = 8.30 (7)°]. In the crystal, supramolecular layers parallel to (10$\bar{5}$) are sustained by nitrobenzene-C—H···O(carbonyl) and pyrrole-C—H···O(nitro) interactions. The layers are connected into a three-dimensional architecture by π(pyrrole)–π(nitrobenzene) stacking [inter-centroid separation = 3.7414 (10) Å] and nitro-O···π(pyrrole) interactions.

1. Chemical context

Many hydroxylated prolines and homoprolines have the ability to inhibit glycosides and glycosyltransferases, key enzymes in biosynthesis and the processing of glycoproteins and glycolipids (Rule *et al.*, 1985; Fleet & Son, 1988; Wong, 1997). Glycoproteins are macromolecules involved in the recognition (cell–cell interactions and host–pathogen) and control of mechanisms associated with biological structures. Thus, compounds that are capable of inhibiting the biosynthetic pathway of glycoproteins have broad chemotherapeutic potential in the treatment of metabolic diseases such as diabetes, obesity, cancer, tuberculosis and viral infections among others (Kordik & Reitz, 1999; Nishimura, 2003; Cheng & Josse, 2004). Some hydroxylated prolines are of interest in this context owing to their ability to inhibit glycosidases and because they are found as substructures of natural bioactive compounds. For example, (2S,3R,4S)-3,4-dihydroxyproline (II), see scheme, is found as a component of the repeating decapeptide sequence of the Mefp1 adhesive protein (Mytilus edulis foot protein 1), produced by the marine mussel, Mytilus edulis (Taylor *et al.*, 1994; Taylor & Weir, 2000). This protein is responsible for the fixation of mussels to rocks. As a part of a study into the development of new and flexible methodologies for the efficient synthesis of several natural and synthetic products with important pharmacological properties, using the Heck–Matsuda arylation reaction as a crucial step, (II) was prepared from the title compound, (I), for the purpose of
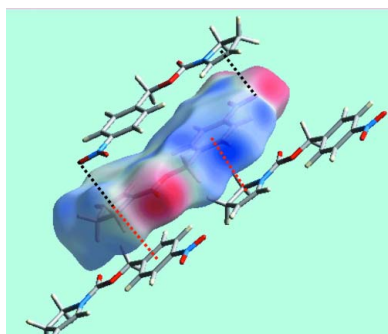
evaluating the best protecting group for use in future syntheses of greater complexity (Garcia, 2008). During the Heck–Matsuda reaction, it was found that the protective group of the nitrogen atom in (I) exerted some influence on the reaction time, but did not influence the yield of the expected intermediate when compared to the Heck–Matsuda reaction applied to the enecarbamate, ethyl 2,3-dihydro-1H-pyrrole-1-carboxylate (Garcia, 2008). It is noted that the first synthesis of (I) was actually reported nearly 50 years ago (Heine & Mente, 1971). Herein, the crystal and molecular structures of (I) are described along with an analysis of the calculated Hirshfeld surfaces.
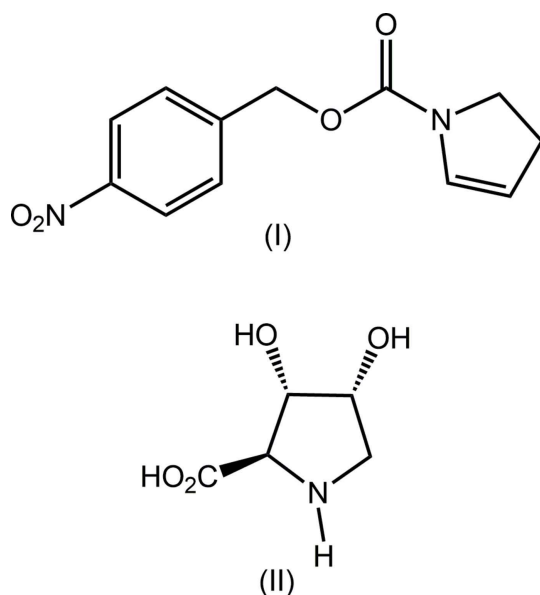
2. Structural commentary

The molecular structure of (I), Fig. 1, is a 1-methylene-4-nitrobenzene ester derived from dihydropyrrole-1-carboxylic acid. In (I), the dihydropyrrole ring is almost planar with the r.m.s. deviation of the five fitted atoms being 0.0049 Å, and the maximum deviation of any of the constituent atoms being 0.0065 (11) Å for atom C2. The adjacent C_2O_2 residue (O1,O2,C5,C6) is essentially co-planar, with the dihedral angle between the two planes being 4.56 (9)°. The planarity extends
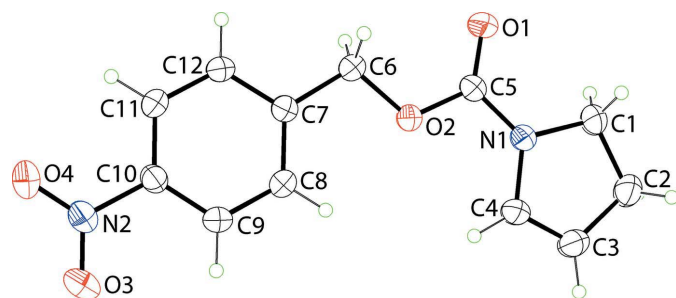
Table 1
Hydrogen-bond geometry (Å, °).

$Cg1$ is the centroid of the N1/C1–C4 ring.

$D—H\cdots A$	$D—H$	$H\cdots A$	$D\cdots A$	$D—H\cdots A$
C4—H4$\cdots$O3[i]	0.93	2.40	3.227 (2)	149
C12—H12$\cdots$O1[ii]	0.93	2.47	3.318 (2)	152
N2—O4$\cdots Cg1$[iii]	1.22 (1)	3.42 (1)	3.6327 (16)	90 (1)

Symmetry codes: (i) $-x+\frac{1}{2}, y-\frac{1}{2}, -z+\frac{1}{2}$; (ii) $-x+2, -y+1, -z+1$; (iii) $-x+1, -y+1, -z+1$.

to the 4-nitrobenzene ring, with the dihedral angle between the C_2O_2 and C_6 planes being 4.58 (8)°. However, the molecule is not planar but rather is curved as the outer rings lie to the same side of the central C_2O_2 residue; the dihedral angle = 8.30 (7)°. To a first approximation, the nitro group is co-planar

(a)

(b)
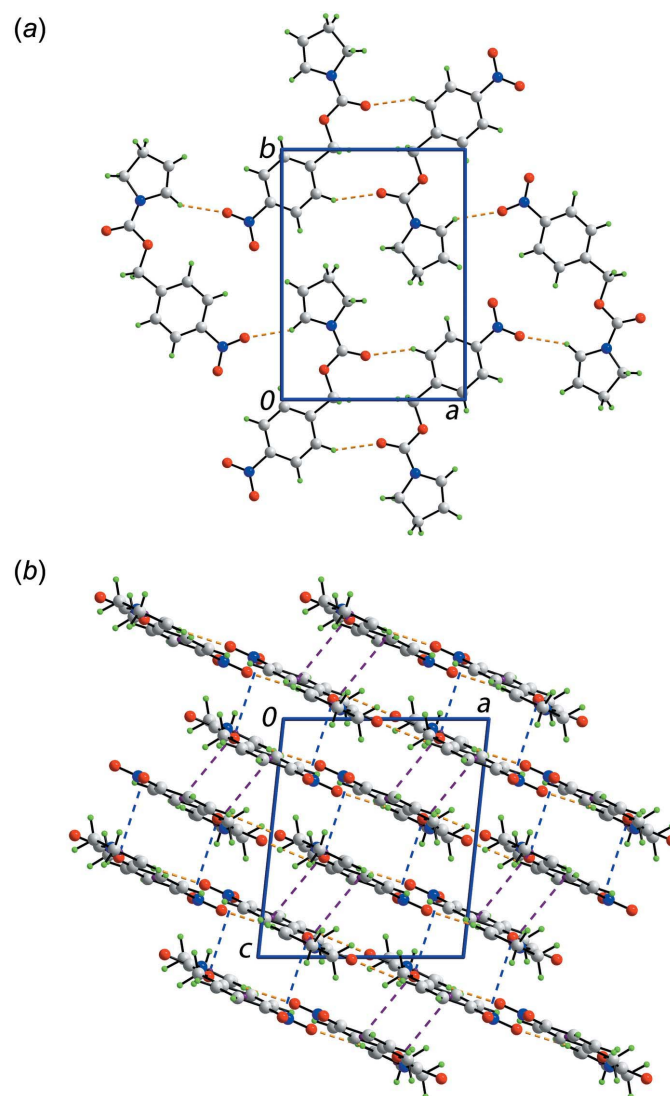
Figure 2
Molecular packing in (I): (a) view of the supramolecular layer parallel to (10$\bar{5}$) plane and (b) view of the unit-cell contents shown in projection down the b axis. The C—H$\cdots$O, N—O$\cdots\pi$ and π–π contacts are shown as orange, blue and purple dashed lines, respectively.

(I)

(II)

Figure 1
The molecular structure of (I), showing the atom-labelling scheme and displacement ellipsoids at the 35% probability level.

with the benzene ring to which is connected, as seen in the value of the O4—N2—C10—C9 torsion angle of 173.50 (15)°.

3. Supramolecular features

The molecular packing of (I) features a variety of directional interactions, Table 1. Thus, nitrobenzene-C12—H···O1(carbonyl) interactions occur over a centre of inversion and lead to 14-membered {···HC$_3$OCO}$_2$ synthons. The dimeric aggregates are connected into a supramolecular layer *via* pyrrole-C4—H···O3(nitro) interactions. The layers lie parallel to (10$\bar{5}$), Fig. 2a. Two types of interactions connect layers into a three-dimensional architecture.Thus, π(N1,C1–C4)–π(C7–C12)^i stacking interactions occur between pyrrole and nitrobenzene rings: inter-centroid separation = 3.7414 (10) Å and angle of inclination = 7.99 (9)° for symmetry code: (i): $\frac{3}{2}$ − x, −$\frac{1}{2}$ + y, $\frac{1}{2}$ − z. The other interactions between layers are of the type nitro-O4···π(N1,C1–C4),

Table 1. These interactions are well known in consolidating the packing of nitro-containing compounds (Huang *et al.*, 2008). A view of the unit-cell contents is shown in Fig. 2b.

4. Hirshfeld surface analysis

The Hirshfeld surface calculations for (I) were performed as per a recent study (Zukerman-Schpector *et al.*, 2017) and serve to provide additional information on the molecular packing.

In addition to the bright-red spots on the Hirshfeld surface mapped over d_{norm} in Fig. 3 near the pyrrole-H4, nitrobenzene-H12, and the nitro-O3 and carbonyl-O1 atoms,

(a)

(b)
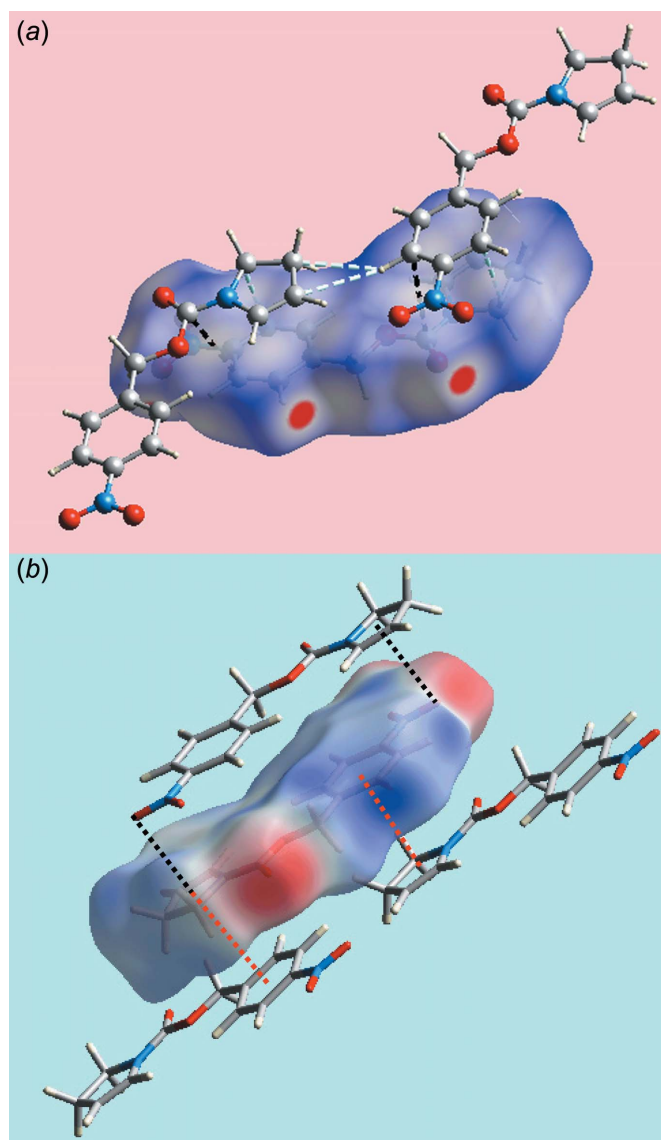
Figure 4
Views of Hirshfeld surfaces for (I) mapped: (a) over d_{norm} in the range −0.225 to + 1.393 au, highlighting inter- and intra-layer C···C and C···H/H···C contacts as black and sky-blue dashed lines, respectively, and (b) over the electrostatic potential in the range ±0.077 au (the red and blue regions represent negative and positive electrostatic potentials, respectively), showing intermolecular N—O···π and π–π contacts as black dotted lines.
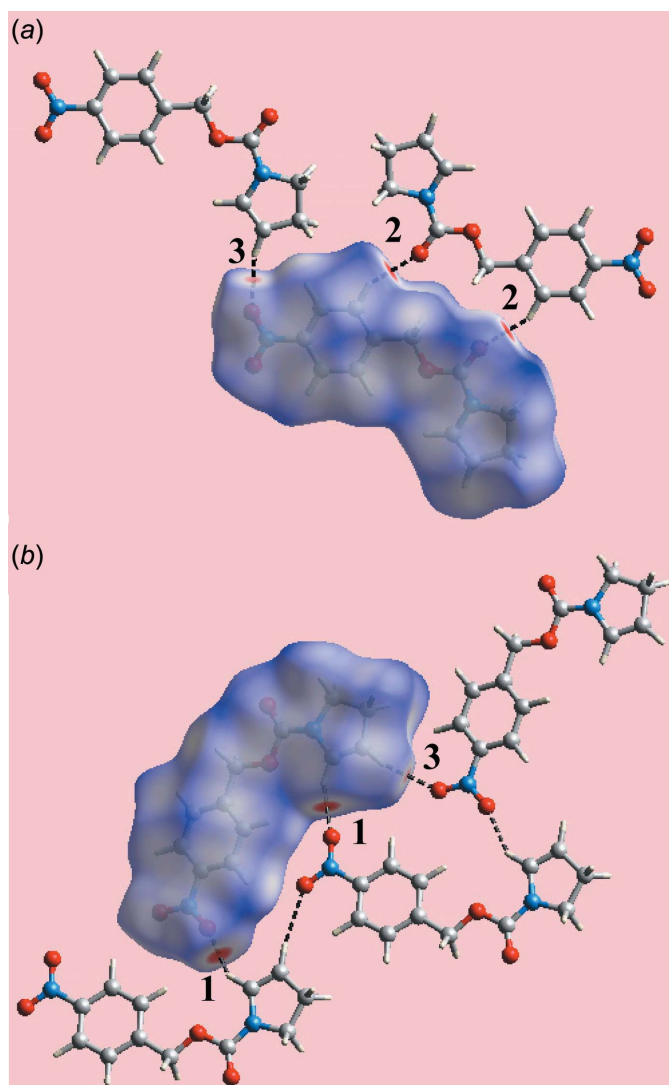
(a)

(b)

Figure 3
Two views of the Hirshfeld surface for (I) mapped over d_{norm} in the range −0.225 to +1.393 au, showing intermolecular C—H···O contacts as black dashed lines.

Table 2
Summary of short interatomic contacts (Å) in (I).

Contact	Distance	Symmetry operation
O4···H3	2.47	$x, -1 + y, z$
C5···C11	3.37	$\frac{3}{2} - x, -\frac{1}{2} + y, \frac{1}{2} - z$
C2···H11	2.81	$x, -1 + y, z$
C3···H11	2.91	$x, -1 + y, z$
C9···H1B	2.92	$\frac{3}{2} - x, \frac{1}{2} + y, \frac{1}{2} - z$

Table 3
Percentage contributions of interatomic contacts to the Hirshfeld surface for (I).

Contact	Percentage contribution
H···H	39.0
O···H/H···O	33.8
C···H/H···C	15.2
C···O/O···C	3.7
C···C	2.4
C···N/N···C	1.7
O···O	1.4
N···H/H···N	1.0
N···O/O···N	0.9
N···N	0.9

representing the respective donors and acceptors of inter-molecular C—H···O interactions (labelled '1' and '2'), the diminutive red spots appearing near the pyrrole-H3 and nitro-O4 atoms in Fig. 3 (labelled '3') also indicate the influence of comparatively weak C—H···O contacts in the crystal (Table 2). The nitrobenzene-C9 and C11 atoms form inter-layer short C···H/H···C and C···C contacts (Table 2) with the pyrrole-H1B and ester-C5 atoms, respectively, Fig. 4a. The other short interatomic C···H/H···C contacts between the nitrobenzene-H11 and pyrrole-C2 and C3 atoms (Table 2) are intra-layer, Fig. 4a. The building up of the three-dimensional architecture through π–π-stacking interactions and nitro-N—O···π(pyrrole) contacts is highlighted in Fig. 4b, showing the Hirshfeld surface mapped over the electrostatic potential.

The overall two-dimensional fingerprint plot and those delineated into H···H, O···H/H···O and C···H/H···C contacts (McKinnon *et al.*, 2007) are illustrated in Fig. 5a–d, respectively, and the percentage contribution from the iden-tified interatomic contacts to the Hirshfeld surface are summarized in Table 3. The comparatively low, *i.e.* 39.0%, contribution from H···H contacts to the overall surface is due to the involvement of many hydrogen atoms in directional intermolecular interactions, *e.g.* C—H···O, π (Tables 1 and 2). Hence, the interatomic H···H contacts have a reduced influ-ence in the crystal as their interatomic separations are equal to or greater than sum of their van der Waals radii (Fig. 5b). Conversely, the relatively significant contribution of 33.8% from O···H/H···O contacts to the Hirshfeld surface is consistent with this observation. The fingerprint plot deli-neated into O···H/H···O contacts (Fig. 5c) features a pair of green aligned points within the pair of spikes with their tips at $d_e + d_i \sim 2.3$ Å superimposed upon a distribution blue points characterizing intermolecular C—H···O interactions. The short interatomic C···H/H···C contacts in the inter- and intra-

layer regions are represented by the two pairs of short forceps-like spikes at $d_e + d_i \sim 2.8$ and 2.9 Å, respectively, in Fig. 5d. The small but discernible contributions from interatomic C···C and C···N/N···C contacts (Table 3) result from short inter-layer contacts and π–π stacking interactions. The presence of the N—O···π contact in the structure is also evident from the contribution of C···O/O···C and N···O/O···N contacts to the Hirshfeld surface as summarized in Table 3. The small contributions from the other remaining interatomic contacts (Table 3) have a negligible influence on the packing.

5. Database survey

Dihydropyrrole rings as found in (I) have rarely been char-acterized crystallographically and only one structure is deposited in the Cambridge Structural Database (Groom *et al.*, 2016), namely the adduct, $ZnI_2(4,5$-dihydro-3H-pyrrole)$_2$ (refcode WAZXAW; Freer *et al.*, 1993). Here, despite having sp^2-carbon centres as in (I), the rings are planar with one lying on a crystallographic mirror plane and the other disposed across a mirror plane (r.m.s. deviation = 0.007 Å), implying disorder in the latter.

6. Synthesis and crystallization

A solution of (4-nitrophenyl)methyl 2-hydroxypyrrolidine-1-carboxylate (2.85 g, 10.704 mmol) in toluene (100 ml) was cooled to 273 K in an ice/water bath. Under an atmosphere of
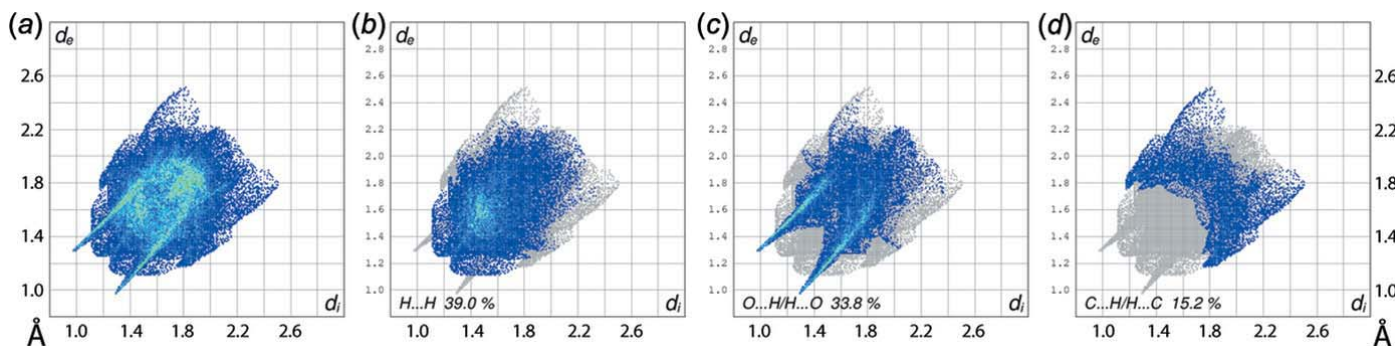

Figure 5
(a) The full two-dimensional fingerprint plot for (I) and those delineated into (b) H···H, (c) O···H/H···O and (d) C···H/H···C contacts.

nitrogen, 2,4-lutidine (6.2 ml, 53.634 mmol) was added to this solution. The solution was stirred for 15 min at 273 K. A trifluoroacetic anhydride (TFAA) solution (13.2 ml of a 0.8 M solution, 10.56 mmol) in dry toluene was then added. The bath was removed and the solution stirred for 2 h at room temperature. Subsequently, the flask was immersed for 20 min in an oil bath preheated to 393–403 K with a reflux condenser. The solution was concentrated in a rotary evaporator and the residue was purified by flash column chromatography on silica gel, using a mixture of EtOAc/n-hexane (1:4) as the eluent. The yield of (I) was 2.103 g (80% based on TFAA). Irregular yellow crystals of (I) were obtained from the slow evaporation of its CH_2Cl_2 solution.

Spectroscopic characterization. ^{1}H NMR (300 MHz, Py-d_5, solution comprises rotamers): δ 8.21 (apparent d, J = 7.3 Hz, 2H, H3′ and H5′), 7.54 (d, J = 8.1 Hz, 2H, H2′ and H6′), 6.80 and 6.68 (2 × m, 1H, H2), 5.35 (s, 2H, CH$_2$), 5.03 (m, 1H, H3), 3.71 (apparent t, J = 9.5 Hz, 2H, H5a,5b), 2.46 (apparent quint., J = 9.5 Hz, 2H, H4a,4b). ^{13}C NMR (75 MHz, Py-d_5, solution comprises rotamers): δ = 152.3 (CO$_2$$R$), 151.5 (CO$_2$$R$), 147.8 (C4′), 144.9 (C1′), 129.8 (C2), 129.2 (C2), 128.4 (C2′ and C6′), 128.3 (C2′ and C6′), 123.9 (C3′ and C5′), 109.4 (C3), 65.8 (CH$_2$), 65.6 (CH$_2$), 45.8 (C5), 45.4 (C5), 30.1 (C4), 29.0 (C4). ESI–MS (m/z) calculated for $C_{12}H_{12}N_2O_4$ 248.07971, found 248.07876.

7. Refinement details

Crystal data, data collection and structure refinement details are summarized in Table 4. The carbon-bound H atoms were placed in calculated positions (C—H = 0.93–0.97 Å) and were included in the refinement in the riding-model approximation, with U_{iso}(H) set to 1.2U_{eq}(C).

References

Brandenburg, K. (2006). *DIAMOND*. Crystal Impact GbR, Bonn, Germany.
Bruker (2009). *APEX2* and *SAINT*. Bruker AXS Inc., Madison, Wisconsin, USA.
Burla, M. C., Caliandro, R., Carrozzini, B., Cascarano, G. L., Cuocci, C., Giacovazzo, C., Mallamo, M., Mazzone, A. & Polidori, G. (2015). *J. Appl. Cryst.* **48**, 306–309.
ChemAxon (2010). *Marvinsketch.* http://www.chemaxon.com.
Cheng, A. Y. Y. & Josse, R. G. (2004). *Drug Discov. Today: Therapeut. Strat.* **1**, 201–206.

Table 4
Experimental details.

Crystal data	
Chemical formula	$C_{12}H_{12}N_2O_4$
M_r	248.24
Crystal system, space group	Monoclinic, $P2_1/n$
Temperature (K)	290
a, b, c (Å)	9.0385 (3), 12.2518 (4), 10.5452 (3)
β (°)	96.102 (1)
V (Å^3)	1161.14 (6)
Z	4
Radiation type	Mo $K\alpha$
μ (mm^{-1})	0.11
Crystal size (mm)	$0.52 \times 0.22 \times 0.14$
Data collection	
Diffractometer	Bruker APEXII CCD
Absorption correction	Multi-scan (*SADABS*; Sheldrick, 1995)
$T_{\min}$, $T_{\max}$	0.724, 0.745
No. of measured, independent and observed [$I > 2\sigma(I)$] reflections	23727, 2394, 2013
R_{int}	0.023
$(\sin \theta/\lambda)_{\max}$ (Å^{-1})	0.627
Refinement	
$R[F^2 > 2\sigma(F^2)]$, $wR(F^2)$, S	0.041, 0.117, 1.09
No. of reflections	2394
No. of parameters	163
H-atom treatment	H-atom parameters constrained
$\Delta\rho_{\max}$, $\Delta\rho_{\min}$ (e Å^{-3})	0.16, −0.18

Computer programs: *APEX2* and *SAINT* (Bruker, 2009), *SIR2014* (Burla *et al.*, 2015), *SHELXL2014* (Sheldrick, 2015), *ORTEP-3 for Windows* (Farrugia, 2012), *DIAMOND* (Brandenburg, 2006), *MarvinSketch* (ChemAxon, 2010) and *publCIF* (Westrip, 2010).

Farrugia, L. J. (2012). *J. Appl. Cryst.* **45**, 849–854.
Fleet, G. W. J. & Son, J. C. (1988). *Tetrahedron*, **44**, 2637–2647.
Freer, A. A., McDermott, G., Melville, J. C. & Robins, D. J. (1993). *Acta Cryst.* C**49**, 2115–2117.
Garcia, A. L. L. (2008). Ph. D. Thesis, Universidade Estadual de Campinas, UNICAMP, Campinas, SP, Brazil.
Groom, C. R., Bruno, I. J., Lightfoot, M. P. & Ward, S. C. (2016). *Acta Cryst.* B**72**, 171–179.
Heine, H. W. & Mente, P. G. (1971). *J. Org. Chem.* **36**, 3076–3078.
Huang, L., Massa, L. & Karle, J. (2008). *Proc. Natl Acad. Sci.* **105**, 13720–13723.
Kordik, C. P. & Reitz, A. B. (1999). *J. Med. Chem.* **42**, 181–201.
McKinnon, J. J., Jayatilaka, D. & Spackman, M. A. (2007). *Chem. Commun.* pp. 3814–3816.
Nishimura, Y. (2003). *Curr. Top. Med. Chem.* **3**, 575–591.
Rule, C. J., Wurzburg, B. A. & Ganem, B. (1985). *Tetrahedron Lett.* **26**, 5379–5380.
Sheldrick, G. M. (1995). *SADABS*. University of Göttingen, Germany.
Sheldrick, G. M. (2015). *Acta Cryst.* C**71**, 3–8.
Taylor, S. W., Waite, J. H., Ross, M. M., Shabanowitz, J. & Hunt, D. F. (1994). *J. Am. Chem. Soc.* **116**, 10803–10804.
Taylor, C. M. & Weir, C. A. (2000). *J. Org. Chem.* **65**, 1414–1421.
Westrip, S. P. (2010). *J. Appl. Cryst.* **43**, 920–925.
Wong, C.-H. (1997). *Pure & Appl. Chem.* **69**, 419–422.
Zukerman-Schpector, J., Sugiyama, F. H., Garcia, A. L. L., Correia, C. R. D., Jotani, M. M. & Tiekink, E. R. T. (2017). *Acta Cryst.* E**73**, 1218–1222.

(4-Nitrophenyl)methyl 2,3-dihydro-1*H*-pyrrole-1-carboxylate: crystal structure and Hirshfeld analysis

Julio Zukerman-Schpector, Monica Soto-Monsalve, Regina H. De Almeida Santos, Ariel L. L. Garcia, Carlos Roque D. Correia, Mukesh M. Jotani and Edward R. T. Tiekink

Computing details

Data collection: *APEX2* (Bruker, 2009); cell refinement: *SAINT* (Bruker, 2009); data reduction: *SAINT* (Bruker, 2009); program(s) used to solve structure: *SIR2014* (Burla *et al.*, 2015); program(s) used to refine structure: *SHELXL2014* (Sheldrick, 2015); molecular graphics: *ORTEP-3 for Windows* (Farrugia, 2012) and *DIAMOND* (Brandenburg, 2006); software used to prepare material for publication: *MarvinSketch* (ChemAxon, 2010) and *publCIF* (Westrip, 2010).

(4-Nitrophenyl)methyl 2,3-dihydro-1*H*-pyrrole-1-carboxylate

Crystal data

$C_{12}H_{12}N_2O_4$	$F(000) = 520$
$M_r = 248.24$	$D_x = 1.420$ Mg m^{-3}
Monoclinic, $P2_1/n$	Mo $K\alpha$ radiation, $\lambda = 0.71073$ Å
$a = 9.0385$ (3) Å	Cell parameters from 9984 reflections
$b = 12.2518$ (4) Å	$\theta = 2.6–26.5°$
$c = 10.5452$ (3) Å	$\mu = 0.11$ mm^{-1}
$\beta = 96.102$ (1)°	$T = 290$ K
$V = 1161.14$ (6) Å^3	Irregular, yellow
$Z = 4$	$0.52 \times 0.22 \times 0.14$ mm

Data collection

Bruker APEXII CCD diffractometer	2394 independent reflections
	2013 reflections with $I > 2\sigma(I)$
φ and ω scans	$R_{int} = 0.023$
Absorption correction: multi-scan (SADABS; Sheldrick, 1995)	$\theta_{max} = 26.5°$, $\theta_{min} = 2.6°$
	$h = -9 \rightarrow 11$
$T_{min} = 0.724$, $T_{max} = 0.745$	$k = -15 \rightarrow 15$
23727 measured reflections	$l = -13 \rightarrow 13$

Refinement

Refinement on F^2	Hydrogen site location: inferred from neighbouring sites
Least-squares matrix: full	H-atom parameters constrained
$R[F^2 > 2\sigma(F^2)] = 0.041$	$w = 1/[\sigma^2(F_o^2) + (0.0501P)^2 + 0.3399P]$ where $P = (F_o^2 + 2F_c^2)/3$
$wR(F^2) = 0.117$	
$S = 1.09$	$(\Delta/\sigma)_{max} < 0.001$
2394 reflections	$\Delta\rho_{max} = 0.16$ e Å^{-3}
163 parameters	$\Delta\rho_{min} = -0.18$ e Å^{-3}
0 restraints	

Special details

Geometry. All esds (except the esd in the dihedral angle between two l.s. planes) are estimated using the full covariance matrix. The cell esds are taken into account individually in the estimation of esds in distances, angles and torsion angles; correlations between esds in cell parameters are only used when they are defined by crystal symmetry. An approximate (isotropic) treatment of cell esds is used for estimating esds involving l.s. planes.

Fractional atomic coordinates and isotropic or equivalent isotropic displacement parameters (Å^2)

	x	y	z	$U_{iso}*/U_{eq}$
O1	0.95640 (13)	0.32527 (10)	0.51064 (14)	0.0665 (4)
O2	0.73098 (11)	0.38092 (8)	0.41873 (11)	0.0489 (3)
O3	0.20267 (15)	0.75353 (13)	0.19648 (17)	0.0896 (5)
O4	0.34938 (16)	0.88645 (10)	0.24771 (15)	0.0720 (4)
N1	0.77129 (13)	0.20438 (10)	0.45899 (13)	0.0468 (3)
N2	0.32222 (15)	0.78902 (12)	0.24108 (13)	0.0532 (3)
C1	0.86033 (17)	0.10688 (13)	0.49447 (17)	0.0514 (4)
H1A	0.8888	0.1046	0.5858	0.062*
H1B	0.9495	0.1052	0.4508	0.062*
C2	0.75720 (19)	0.01184 (14)	0.45210 (19)	0.0581 (4)
H2A	0.7987	−0.0322	0.3881	0.070*
H2B	0.7401	−0.0342	0.5239	0.070*
C3	0.61637 (18)	0.06612 (14)	0.39787 (18)	0.0558 (4)
H3	0.5308	0.0292	0.3652	0.067*
C4	0.62960 (16)	0.17304 (13)	0.40258 (16)	0.0505 (4)
H4	0.5549	0.2216	0.3725	0.061*
C5	0.83046 (16)	0.30513 (12)	0.46670 (15)	0.0443 (3)
C6	0.78181 (17)	0.49186 (12)	0.42996 (17)	0.0490 (4)
H6A	0.8665	0.5019	0.3819	0.059*
H6B	0.8127	0.5089	0.5186	0.059*
C7	0.65706 (15)	0.56621 (11)	0.37923 (13)	0.0400 (3)
C8	0.51427 (16)	0.52938 (12)	0.33957 (14)	0.0442 (3)
H8	0.4927	0.4553	0.3436	0.053*
C9	0.40373 (17)	0.60201 (12)	0.29406 (15)	0.0445 (3)
H9	0.3082	0.5774	0.2672	0.053*
C10	0.43818 (16)	0.71143 (12)	0.28935 (13)	0.0414 (3)
C11	0.57881 (17)	0.75032 (12)	0.32932 (16)	0.0481 (4)
H11	0.5996	0.8246	0.3262	0.058*
C12	0.68753 (17)	0.67727 (12)	0.37385 (16)	0.0478 (4)
H12	0.7828	0.7025	0.4007	0.057*

Atomic displacement parameters (Å^2)

	U^{11}	U^{22}	U^{33}	U^{12}	U^{13}	U^{23}
O1	0.0418 (6)	0.0487 (7)	0.1027 (10)	−0.0039 (5)	−0.0220 (6)	0.0065 (6)
O2	0.0409 (6)	0.0331 (5)	0.0694 (7)	0.0014 (4)	−0.0086 (5)	0.0017 (4)
O3	0.0510 (8)	0.0752 (10)	0.1334 (14)	0.0052 (7)	−0.0338 (8)	0.0061 (9)
O4	0.0699 (9)	0.0433 (7)	0.0990 (10)	0.0135 (6)	−0.0083 (7)	0.0061 (6)
N1	0.0352 (6)	0.0369 (6)	0.0660 (8)	0.0025 (5)	−0.0052 (5)	0.0040 (6)

N2	0.0467 (8)	0.0498 (8)	0.0610 (8)	0.0086 (6)	−0.0039 (6)	0.0025 (6)
C1	0.0442 (8)	0.0408 (8)	0.0681 (10)	0.0078 (6)	0.0017 (7)	0.0066 (7)
C2	0.0561 (10)	0.0417 (8)	0.0766 (11)	0.0010 (7)	0.0070 (8)	0.0059 (8)
C3	0.0440 (8)	0.0476 (9)	0.0752 (11)	−0.0077 (7)	0.0032 (8)	−0.0010 (8)
C4	0.0342 (8)	0.0459 (8)	0.0696 (10)	−0.0006 (6)	−0.0026 (7)	0.0024 (7)
C5	0.0363 (7)	0.0403 (8)	0.0545 (8)	0.0023 (6)	−0.0034 (6)	0.0027 (6)
C6	0.0432 (8)	0.0352 (7)	0.0660 (10)	−0.0034 (6)	−0.0066 (7)	0.0011 (7)
C7	0.0387 (7)	0.0369 (7)	0.0435 (7)	0.0005 (6)	−0.0006 (6)	−0.0008 (6)
C8	0.0447 (8)	0.0347 (7)	0.0519 (8)	−0.0042 (6)	−0.0009 (6)	0.0008 (6)
C9	0.0367 (7)	0.0434 (8)	0.0516 (8)	−0.0046 (6)	−0.0028 (6)	−0.0015 (6)
C10	0.0391 (7)	0.0406 (8)	0.0434 (7)	0.0050 (6)	−0.0007 (6)	−0.0006 (6)
C11	0.0461 (8)	0.0325 (7)	0.0640 (9)	−0.0023 (6)	−0.0019 (7)	−0.0013 (6)
C12	0.0370 (8)	0.0392 (8)	0.0647 (9)	−0.0040 (6)	−0.0056 (7)	−0.0029 (7)

Geometric parameters (Å, º)

O1—C5	1.2080 (18)	C3—H3	0.9300
O2—C5	1.3527 (17)	C4—H4	0.9300
O2—C6	1.4356 (17)	C6—C7	1.503 (2)
O3—N2	1.2123 (18)	C6—H6A	0.9700
O4—N2	1.2193 (18)	C6—H6B	0.9700
N1—C5	1.3442 (19)	C7—C8	1.389 (2)
N1—C4	1.4070 (18)	C7—C12	1.391 (2)
N1—C1	1.4665 (18)	C8—C9	1.385 (2)
N2—C10	1.4656 (19)	C8—H8	0.9300
C1—C2	1.528 (2)	C9—C10	1.378 (2)
C1—H1A	0.9700	C9—H9	0.9300
C1—H1B	0.9700	C10—C11	1.381 (2)
C2—C3	1.495 (2)	C11—C12	1.374 (2)
C2—H2A	0.9700	C11—H11	0.9300
C2—H2B	0.9700	C12—H12	0.9300
C3—C4	1.316 (2)		
C5—O2—C6	115.15 (11)	O1—C5—O2	124.40 (14)
C5—N1—C4	127.92 (13)	N1—C5—O2	111.31 (12)
C5—N1—C1	121.91 (12)	O2—C6—C7	108.85 (12)
C4—N1—C1	109.61 (12)	O2—C6—H6A	109.9
O3—N2—O4	122.62 (15)	C7—C6—H6A	109.9
O3—N2—C10	118.50 (14)	O2—C6—H6B	109.9
O4—N2—C10	118.88 (14)	C7—C6—H6B	109.9
N1—C1—C2	104.18 (12)	H6A—C6—H6B	108.3
N1—C1—H1A	110.9	C8—C7—C12	119.16 (13)
C2—C1—H1A	110.9	C8—C7—C6	123.24 (13)
N1—C1—H1B	110.9	C12—C7—C6	117.59 (12)
C2—C1—H1B	110.9	C9—C8—C7	120.57 (14)
H1A—C1—H1B	108.9	C9—C8—H8	119.7
C3—C2—C1	103.94 (13)	C7—C8—H8	119.7
C3—C2—H2A	111.0	C10—C9—C8	118.68 (13)

C1—C2—H2A	111.0	C10—C9—H9	120.7
C3—C2—H2B	111.0	C8—C9—H9	120.7
C1—C2—H2B	111.0	C9—C10—C11	121.93 (14)
H2A—C2—H2B	109.0	C9—C10—N2	119.17 (13)
C4—C3—C2	110.99 (14)	C11—C10—N2	118.90 (13)
C4—C3—H3	124.5	C12—C11—C10	118.75 (14)
C2—C3—H3	124.5	C12—C11—H11	120.6
C3—C4—N1	111.26 (14)	C10—C11—H11	120.6
C3—C4—H4	124.4	C11—C12—C7	120.90 (13)
N1—C4—H4	124.4	C11—C12—H12	119.5
O1—C5—N1	124.29 (13)	C7—C12—H12	119.5
C5—N1—C1—C2	−171.59 (15)	O2—C6—C7—C12	−175.74 (14)
C4—N1—C1—C2	0.51 (18)	C12—C7—C8—C9	0.6 (2)
N1—C1—C2—C3	−0.98 (18)	C6—C7—C8—C9	179.78 (14)
C1—C2—C3—C4	1.2 (2)	C7—C8—C9—C10	−0.2 (2)
C2—C3—C4—N1	−0.9 (2)	C8—C9—C10—C11	−0.4 (2)
C5—N1—C4—C3	171.74 (16)	C8—C9—C10—N2	179.85 (13)
C1—N1—C4—C3	0.2 (2)	O3—N2—C10—C9	−6.2 (2)
C4—N1—C5—O1	−175.78 (17)	O4—N2—C10—C9	173.50 (15)
C1—N1—C5—O1	−5.2 (3)	O3—N2—C10—C11	174.03 (17)
C4—N1—C5—O2	4.1 (2)	O4—N2—C10—C11	−6.2 (2)
C1—N1—C5—O2	174.65 (14)	C9—C10—C11—C12	0.6 (2)
C6—O2—C5—O1	−3.7 (2)	N2—C10—C11—C12	−179.62 (14)
C6—O2—C5—N1	176.46 (13)	C10—C11—C12—C7	−0.2 (2)
C5—O2—C6—C7	−176.99 (13)	C8—C7—C12—C11	−0.4 (2)
O2—C6—C7—C8	5.1 (2)	C6—C7—C12—C11	−179.60 (15)

Hydrogen-bond geometry (Å, º)

Cg1 is the centroid of the N1/C1–C4 ring.

D—H···A	D—H	H···A	D···A	D—H···A
C4—H4···O3[i]	0.93	2.40	3.227 (2)	149
C12—H12···O1[ii]	0.93	2.47	3.318 (2)	152
N2—O4···Cg1[iii]	1.22 (1)	3.42 (1)	3.6327 (16)	90 (1)

Symmetry codes: (i) −x+1/2, y−1/2, −z+1/2; (ii) −x+2, −y+1, −z+1; (iii) −x+1, −y+1, −z+1.